XIV CONGRESS OF THE INTERNATIONAL SOCIETY FOR PHOTOGRAMMETRY
HAMBURG 1980

COMMISSION III WORKING GROUP 2

P r e s e n t e d P a p e r

by M.Ehlers and B.Wrobel, Hannover

DIGITAL CORRELATION OF REMOTE SENSING IMAGERY FROM TIDAL LANDS

Summary

For correlation of remote sensing photographs of mud-flats a concept for rectification on a mutual reference image was developed in SFB 149. Different target functions show some deviations in the results because of the unstructured topography of the mud-flats. Quality and accuracy of two chosen target functions are presented by examples for autocorrelation as well as unitemporal and multitemporal correlation. A pre-handling of the data by geometric or densitometric treatment is necessary for increasing the available information from the image signals.

1. Introduction

Picture analysis of more than one picture of the same object requires the correlation of homologeous parts in different images. After this fundamental operation one can extract desired information from the images, e.g. semantic information only by picture comparison or information about the geometry of the mapped objects in combination with photogrammetric techniques. For more than 120 years the photogrammetry achieved great successes with these methods - especially with the well-known technique of stereophotogrammetry.

The image-correlation-process is still a fundamental element of the photogrammetric operations - also for the future, but with other than the previous means, namely increasing with digital methods and automatic control (1),(2). That is particularly why these are the suitable means for the evaluation of remote sensing imagery with their specific problems. The user expects fast analysis of many pictures, mainly of those, which are not convenient for the human eye (RADAR, line scanner images with many channels). Of main interest hereby are the problems of rectification and change detection in multitemporal photos. (Table 1)
The correlation process describes a mapping of the density functions of small image parts: the density function $S_2(x'',y'')$ of a search image is mapped on the density function $S_1(x',y')$ of a reference image with respect to radiometric and geometric parameters. Because of the existing stochastic components it is a question of multiple regression analysis to optimize an objective function, e.g. a function of the residues (3).
A large number of objective functions have been used (table 2). The one known best, the correlation function, gave the name to this field of operation.
This topic was picked up at the University of Hannover by the Sonderfor-

schungsbereich (SFB) 149, "Surveying and Remote Sensing Methods at Coasts and Oceans."
In the following the problems of digital image correlation from tidal lands will be discussed.

Table 1: application of digital image correlation

reference image sensor[1]	search image sensor	applications	remarks
RMK	RMK	digital terrain model, orthophotos, stereocompilation point transfer for aerotriangulation	in principle solved
RMK	RMK MSS RADAR	rectification change detection	solvable, in development
line drawing map	RMK MSS RADAR		problematic

1) RMK = aerial camera (Reihenmeßkammer)
MSS = multispectralscanner

Table 2: objective functions used for optimal image matching

A) maximum crosscorrelation:

$$\mathrm{cor}\left\{S_1(x',y'),S_2(x'',y'')\right\} = \max!$$

B) maximum crosscovariance:

$$\mathrm{cov}\left\{S_1(x',y'),S_2(x'',y'')\right\} = \max!$$

C) least squares method (Gauß):

$$\sum\left\{p'\,v^2(x',y')+p''\,v^2(x'',y'')\right\} = \min!$$

D) minimum sum of the absolut values (Laplace):

$$\sum\left|S_1(x',y')-S_2(x'',y'')\right| = \min!$$

E) maximum phase correlation of the cross spectrum from $S_1(x',y')$ with $S_2(x'',y'')$

F) maximum correlation intensity from $S_1(x',y')$ with $S_2(x'',y'')$

2. Groundworks

2.1. Test Area

The test areas of the SFB 149 are the wet zones in the Jadebusen near Wilhelmshaven. Wet zones differ from almost all continental areas mainly in two characteristics:

a) Because of the vanishing differences in height and the extremely flat slope of the terrain one can consider that tidal lands are an even plain. Therefore the correlation algorithm does not need to take notice of changes in height and slope.

b) On the other hand the homogeneous structure of this area is a disadvantage.
The small morphologic and vegetative differences complicate the finding of identical points in different images.

The first illustrations prove the homogeneous structure of tidal lands (fig.1 and 2). Fig.1 shows a onedimensional 2.5 cm section of a RMK-photo (original scale 1:2000), which was digitized with the sampling rate of ΔX = 12.5 µm in 2000 discrete points. Fig.2 shows the power spectrum of this section. The main information is in a small band of low frequencies. The frequencies are normalized on the Nyquist-Frequency $f_N = \frac{1}{20\Delta x} = 40$ lp/mm.

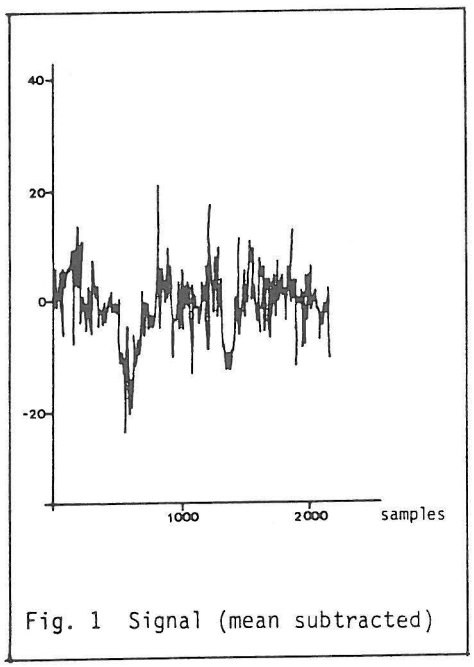

Fig. 1 Signal (mean subtracted)

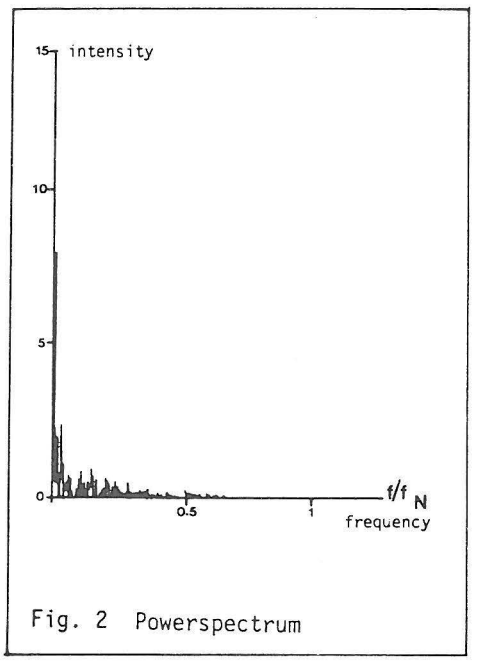

Fig. 2 Powerspectrum

The consideration of this spectral distribution will be the main problem for the construction of correlation agorithms.

2.2. Sensors and Image material

The test area is investigated systematically since 1975 with flight and ground-truth-measurements. Sensors, films and flying heights are presented in table 3.

Table 3:

period of remote sensing mission	sensors [1]	films [2]	flying height in m
august 1975	Hb,RMK	bw,cir,c	300,600
may 1976	Hb,RMK	cir,c	610
august 1976	Hb,RMK,MSS	c,ms	610
september 1978	RMK,MSS	cir,ms	200,400,600,900
october 1979	RMK,MSS, ESLAR	cir,ms	300,600

1) Hb = Hasselblad, ESLAR = Experimental Side Looking Airborne Radar
2) c = colour, cir = colour infrared, bw = black and white, ms = multispectral (on tape)

2.3. Image processing system

For analog/digital-transformation and further evaluation of aerial images the SFB 149 has installed the image processing system schematically shown in fig.3. The part of the diagram, which is bordered by a broken line shows the enlargement of the system to an interactive one. This will be completed this year (3).

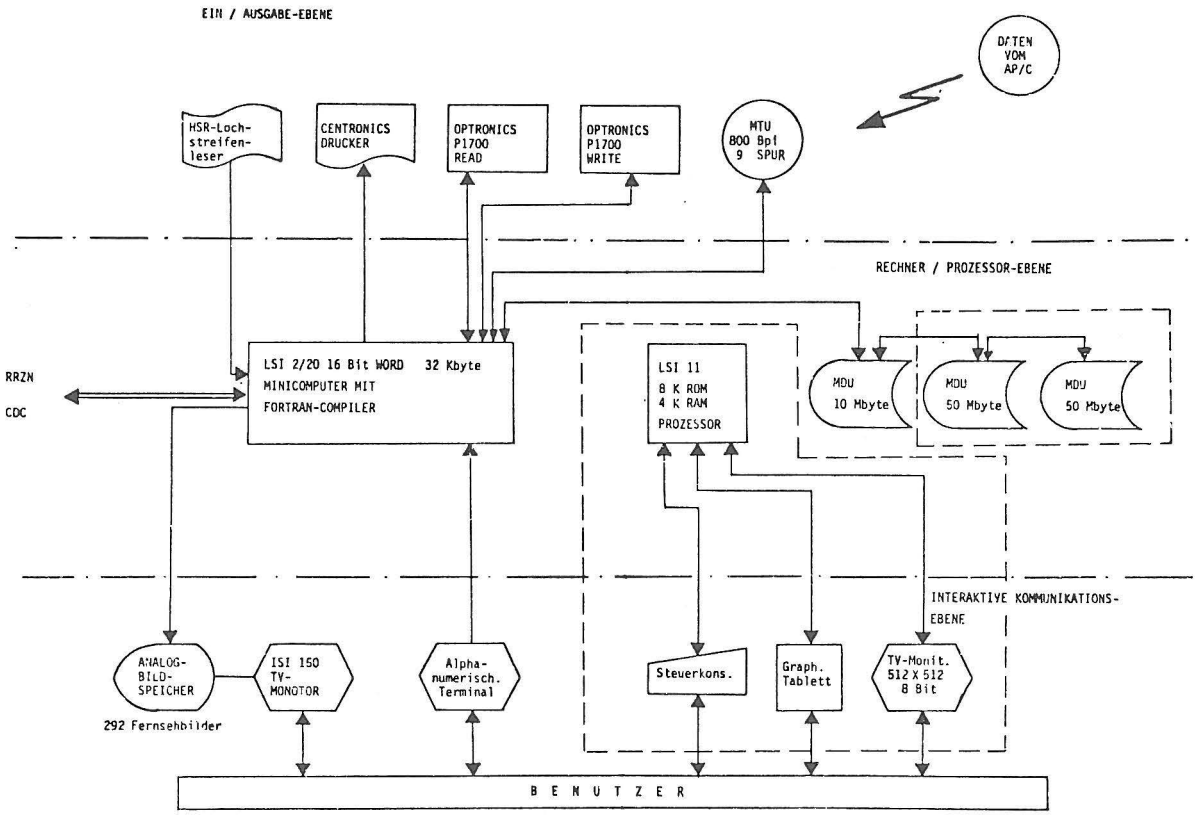

Fig. 3 Image processing system of the SFB 149

3. Correlation algorithm

3.1. Correlation concept

The correlation concept to rectify remote sensing images with respect to a common reference picture has to be as universal as possible because of the homogeneous topography of the research area and the different image sensors. Likewise the user should be able to manipulate interactively the evaluation process to profit by all informations of the correlation process and to influence the decisions. The following diagram outlines this concept. The programs to rectify remote sensing images with respect to pass points do already exist at the SFB 149. Interactive parts of the concept are bordered by a thick line.

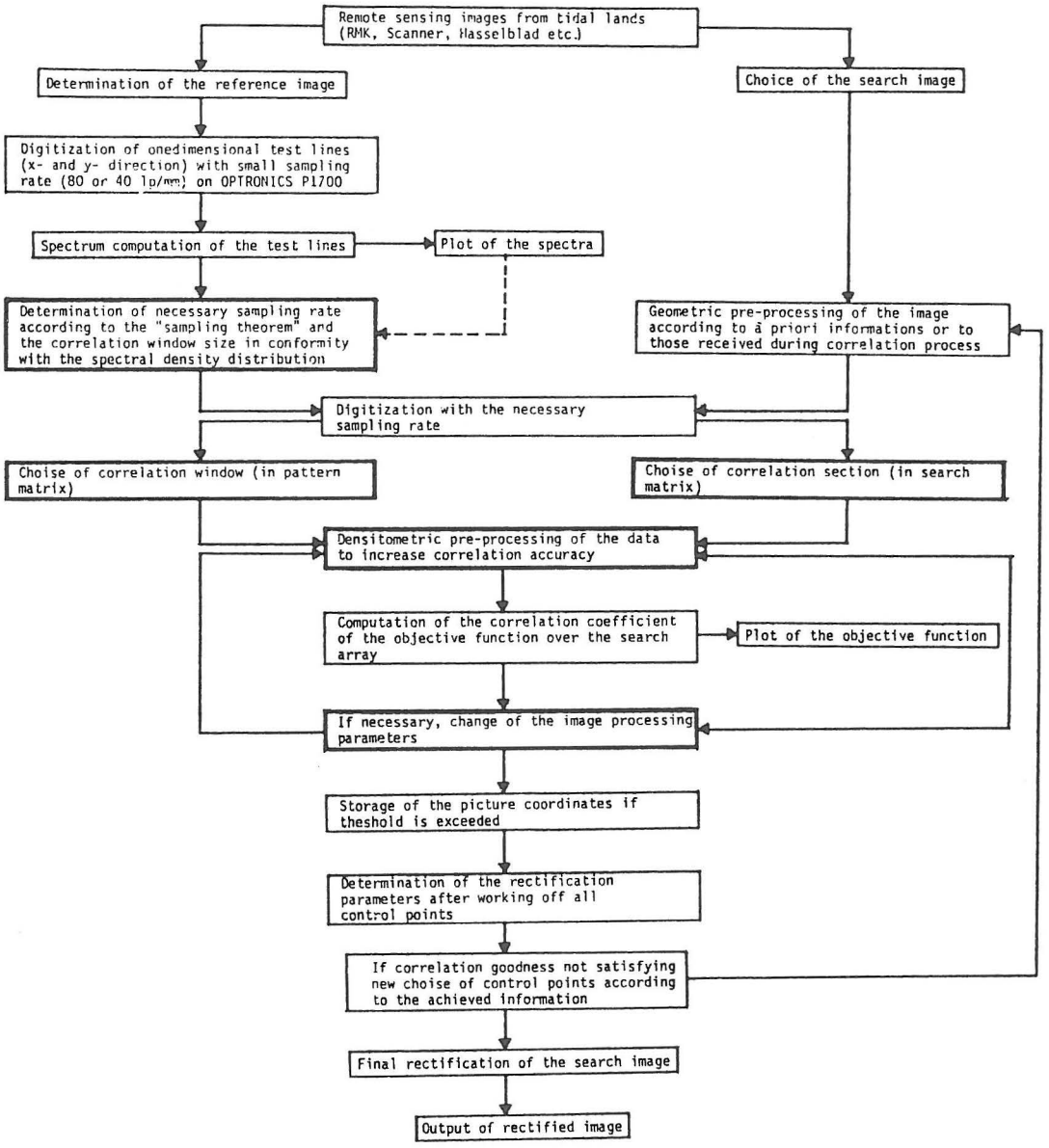

Fig. 4 Correlation concept

3.2. Objective functions

Given are the gray values of the image signals, $S_2(x_i,y_j)$, $i=1,..,N_2$, $j=1,...,M_2$ of the pattern matrix from the reference image and $S_1(x_i,y_j)$, $i=1,..,N_1$, $j=1,..,M_1$ of the search matrix from the search image (both digitized in the range [0,255]). The centre of the pattern matrix gives the coordinates of the control point in the reference image. By shifting the pattern matrix over the search matrix one tries to find the position of greatest similarity. Two of the objective functions shown in the introduction are implementated in the concept.

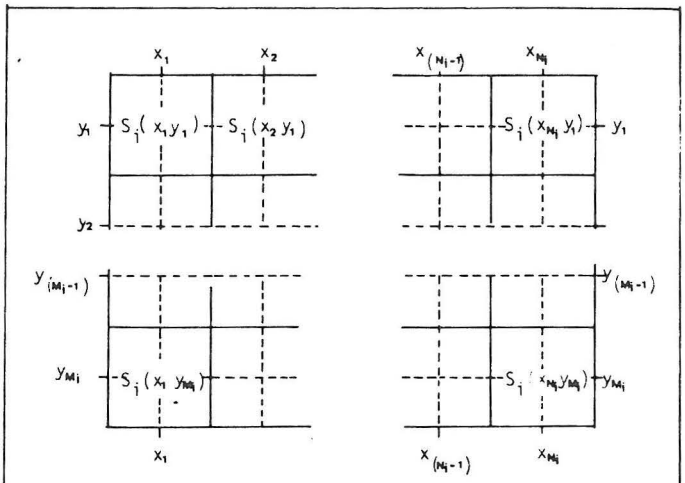

Fig. 5 Structure of search matrix S_1 and pattern matrix S_2
($N_1 >> N_2$ and $M_1 >> M_2$)

a) the product moment correlation coefficient

$$r(\Delta x,\Delta y) = \frac{\sum_{i=1}^{N2}\sum_{j=1}^{M2}\left\{S_1(x_i+\Delta x,y_j+\Delta y)-\bar{S}_1\right\}\cdot\left\{S_2(x_i,y_i)-\bar{S}_2\right\}}{\sum_{i=1}^{N2}\sum_{j=1}^{M2}\left\{S_1(x_i+\Delta x,y_j+\Delta y)-\bar{S}_1\right\}^2 \sum_{i=1}^{N2}\sum_{j=1}^{M2}\left\{S_2(x_iy_j)-\bar{S}_2\right\}^2}$$

with

$$\bar{S}_1 = \frac{1}{M_2\cdot N_2}\sum_{i=1}^{N_2}\sum_{j=1}^{M_2} S_1(x_i+\Delta x,\ y_j+\Delta y)$$

$$\bar{S}_2 = \frac{1}{M_2\cdot N_2}\sum_{i=1}^{N_2}\sum_{j=1}^{M_2} S_2(x_i,y_i)$$

the means of the grey values of the compared matrixes.
$(\Delta x,\Delta y)$ is the shift vector, which specifies the relative position of the pattern in the search matrix.

b) the correlation intensity coefficient

$$I(\Delta x,\Delta y) = \left\{\sum_{i=1}^{N_2}\sum_{j=1}^{M_2} \cos p\left[S_1(x_i+\Delta x,y_j+\Delta y)-S_2(x_i,y_j)\right]\right\}^2$$

$$+\left\{\sum_{i=1}^{N_2}\sum_{j=1}^{M_2} \sin p\left[S_1(x_i+\Delta x,y_j+\Delta y)-S_2(x_i,y_j)\right]\right\}^2$$

normalized on $[0,1]$ with the correlation parameter p, which is derived from the signal variances

$$p = \frac{0.5\,\pi}{\sqrt{\frac{\sum\sum\left\{S_1(x_i+\Delta x,y_j+\Delta y)-\bar{S}_1\right\}^2+\sum\sum\left\{S_2(x_i,y_i)-\bar{S}_2\right\}^2}{M_2\cdot N_2}}}$$

The correlation intensity coefficient was developed out of koherent-optical considerations (4). The image signals are mapped on the complex plane and the intensity of the complex correlation function is computed.
The shift vector of the maximum of both functions gives the most probable position of the pattern matrix in the search image.

4. First results

4.1. Autocorrelation

For testing of the objective functions an area of 200x200 picture elements (pixel) out of RMK-photo was digitized. Submatrices therefrom were chosen as pattern matrices. Fig.6-9 show an example of these results. The pattern

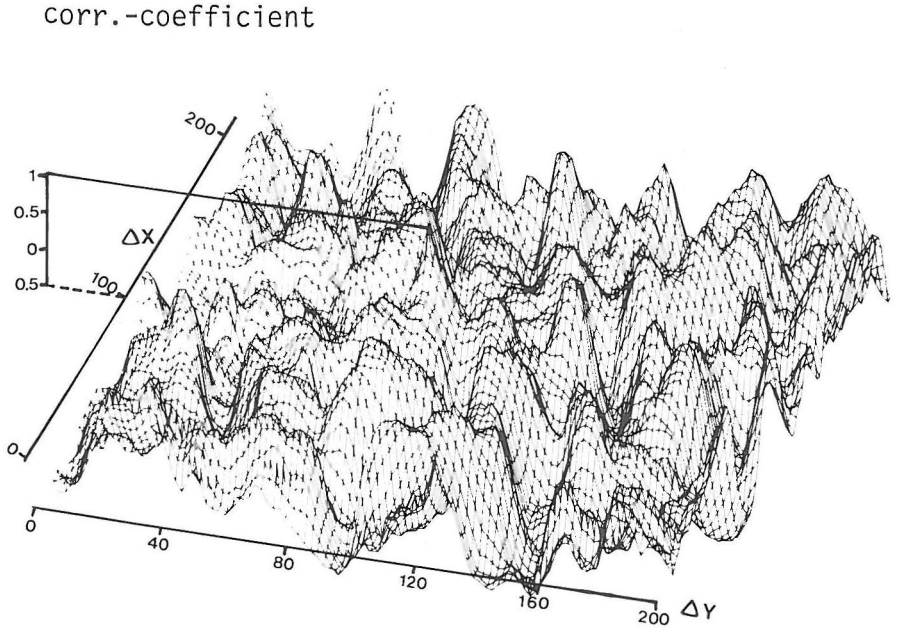

Fig.6 Twodimensional correlation function

matrix was a 15x15 pixel section of the search matrix. Fig.6 and 8 are projections of the twodimensional objective functions and fig.7 and 9 onedimensional cuts therefrom, which include their maxima.
Both functions show the maxim.on the right position, but they differ clearly. The intensity function approximates a δ-function and shows the maximum more sharply than the correlation function (4). This one differs not significantly from 1 in some positions. That is why a clear location of the right reference point is made very difficult already with autocorrelation. Here the complex exponentiation of image data turns out to be advantageous.

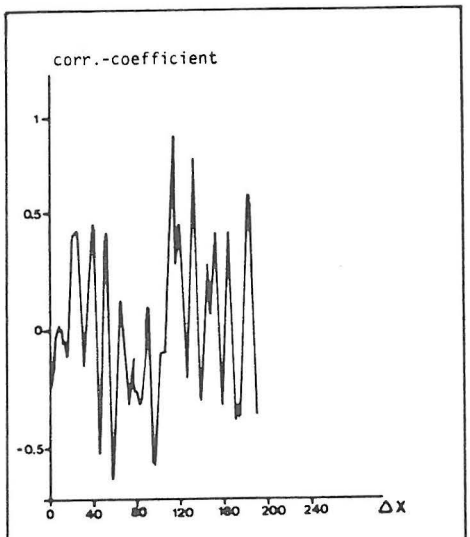

Fig. 7 Correlation function

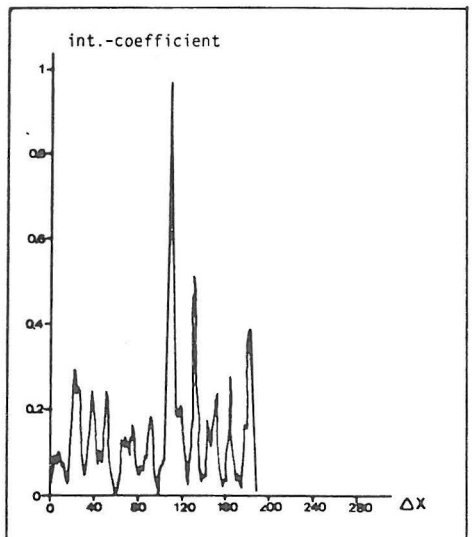

Fig. 9 Intensity function

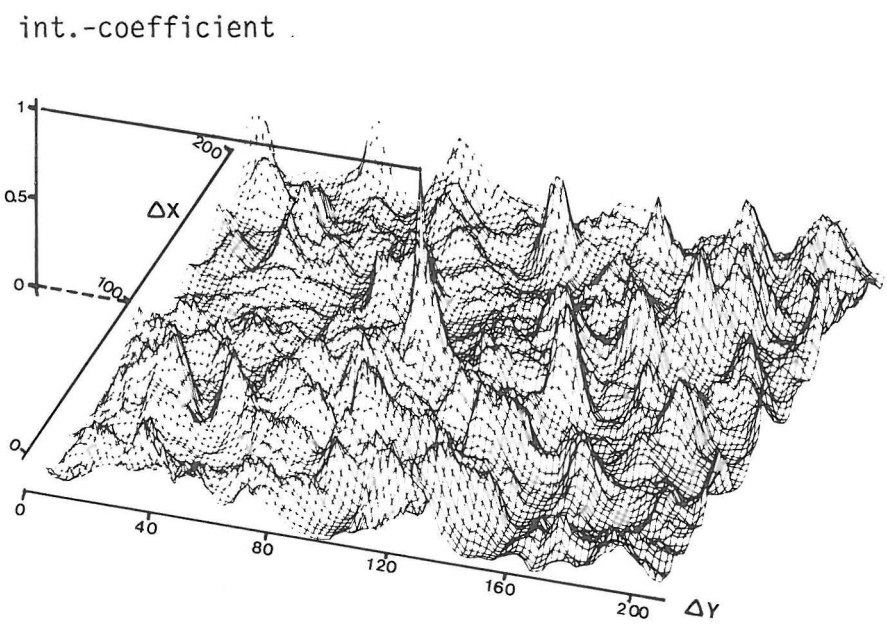

Fig. 8 Twodimensional intensity function

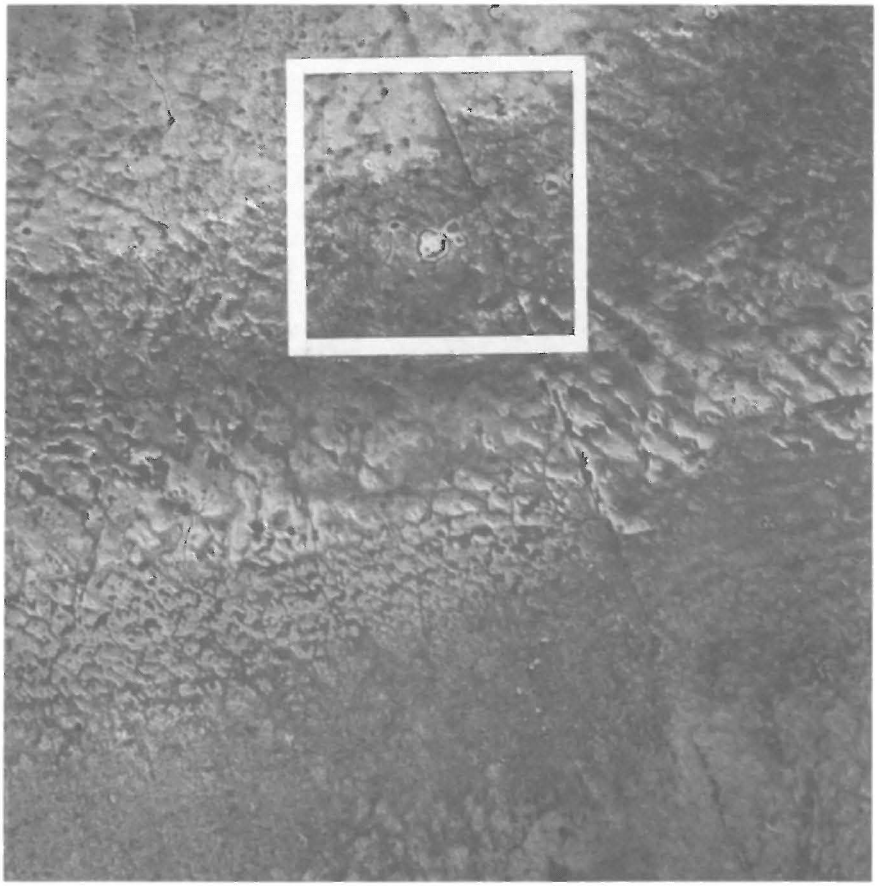

Fig.10 and 11 Aerial camera photographs from 13.8.75

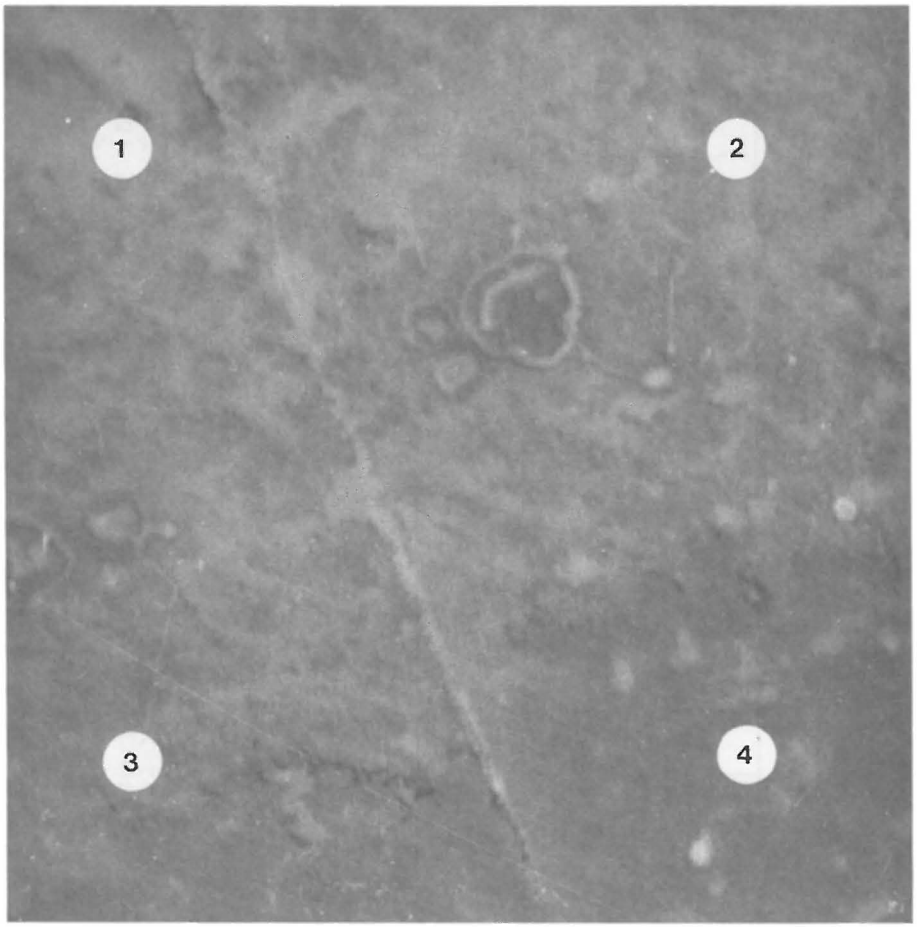

Fig. 12 Reference image with control points

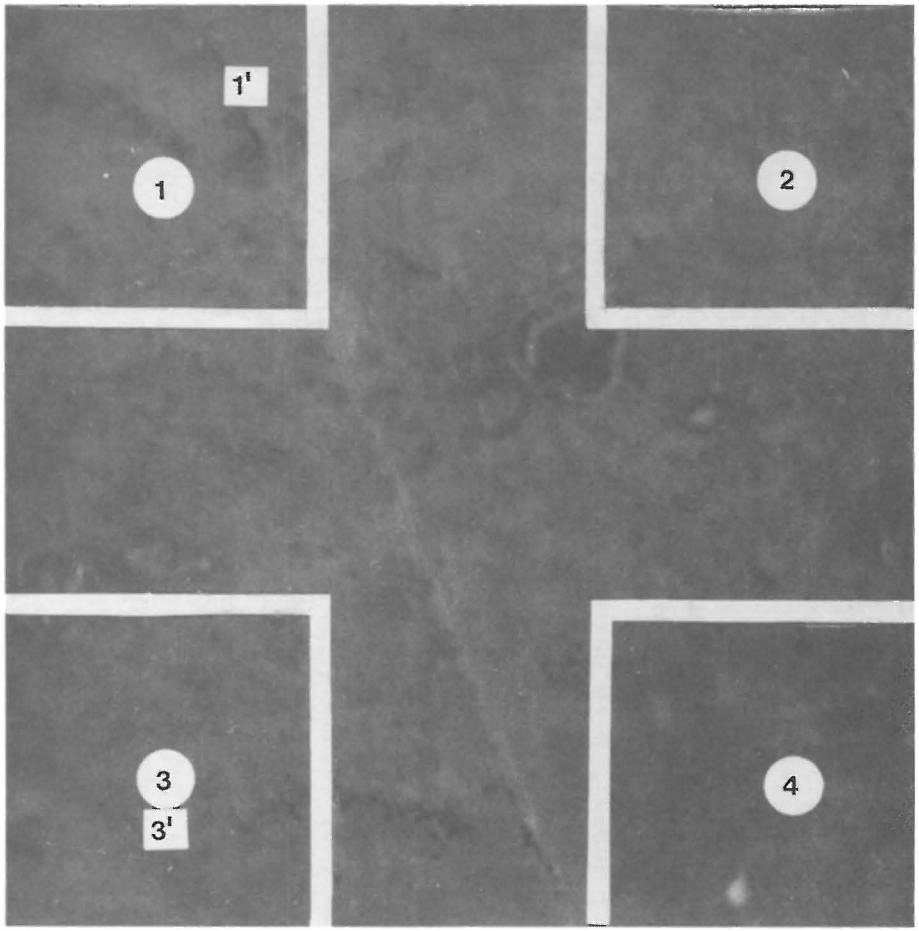

Fig. 13 Search image with search matrices (white borded) positions of correlation coefficient maxima (round) and intensity coefficient maxima (angular)

4.2. Unitemporal crosscorrelation

To test the presented concept with crosscorrelation two overlapping RMK-photos (original scale 1:2000) with relatively high contrast were chosen (fig. 10 and 11). Two almost identical sections were digitized with a sufficiently high sampling rate of 100 µm (≙ 10 lp/min), see fig. 2,12 and 13. Four control points((1) - (4) in fig.12) were selected as centres of four 11x11 pixel pattern matrices. In the corresponding areas of the search image four 100x100 pixel search matrices are determined. Table 4 and fig.13 show the correlation maxima of both functions and the deviations of their positions.

Table 4: correlation maxima

point	r_{max} $-1 \leq r \leq 1$	I_{max} $0 \leq I \leq 1$	deviation of the shift vector (in pixel)	
			Δx	Δy
1	0.755	0.596	32	24
2	0.863	0.660	0	0
3	0.676	0.412	12	2
4	0.951	0.855	1	0

It is surprising that even in those homogenous images (for the human eye) the position parameters deviate in such a way.
It can easily be estimated by the eye that the intensity function fails at point 1 and 3, whereas the correlation function seems to find the control points correctly. Why does the method of complex exponentiation give the wrong results? One reason manifests the power spectrum of the flat land (fig. 2). Almost the entire information is concentrated in the low-frequency range, whereas in the high-frequency ranges the signal-to-noise ratio (SNR) is very small. The complex exponentiation method now normalizes the power spectrum (whitening) (4). Therefore random noise in high frequencies together with a small SNR can be a great source for failures. For that reason it is necessary to investigate whether real information can be separated from random noise by filter techniques or other image preprocessing. Further one can see that at point 1 and 3 the smallest values for r_{MAX} as well as I_{MAX} are computed, so that these values can be expected to give a prediction of the correlation efficiency. Exact statistical determination, however, is a problem and has not yet been sufficiently cleared until now because of the unknown number of degrees of freedom (ndf).

4.3. Multitemporal crosscorrelation

The problems to find identical points in different images with the correlation method increases if the images are taken at different times and with different films. As an example a RMK photo of September 78 with partial vegetation and a RMK false colour photo of May 76 without vegetation were chosen as reference and search image. Six control points or pattern matrices respectively, and search matrices were chosen in the way described in point 4.2. The results are found in table 5.

Table 5: correlation maxima

point	r_{max}	I_{max}	changes in topographic features	deviation of the shift vector Δx	Δy
1	0.569	0.355	yes	0	0
2	0.432	0.235	yes	115	7
3	0.703	0.437	no	0	0
4	0.435	0.495	yes	60	3
5	0.400	0.194	yes	50	20
6	0.624	0.337	no	1	1

As one would expect the values of the correlation maximum are smaller and the deviations of the corresponding shift vectors are greater than they are at unitemporal correlation. But the points with no changes (3 and 6) in the neighbourhood are mapped to the same points by both correlation functions. These points seem to be the right ones by eye-control. Therefore an image pre-rectification with selected good controlpoints together with densitometric image evaluation and a new choice of controlpoints in the prerectified picture should lead to better results.

5. Conclusion and further works

Quality and accuracy of the presented examples for digital correlation show that picture pre-processing (geometric and densitometric) is necessary. The results of unevaluated data do not satisfy, so that also other objective functions should be tested. Filter techniques for optimal signal and noise separation shall be integrated in the correlation system as it is scheduled in 3. after the lining of the image processing system an interactive one. At the same time tests for the goodness of the correlation coefficient shall be developed where the ndf shall be derived from the autocorrelation length. But already the previous results allow the conclusion that digital correlation of aerial images of tidal lands is a useful and effective method for rectification with respect to a reference image, if the above mentioned difficulties can be eliminated.

References

(1) G.L.Hobrough: Digital on-line Correlation, Symposium on the Use of Digital Components in Photogrammetry, Hannover 1978. Wiss.Arbeiten der Lehrstühle Geodäsie, Photogrammetrie und Kartographie Nr.84

(2) B.Wrobel: Geometrische Aspekte der Korrelationssteuerung, see (1)

(3) B.Wrobel and M.Ehlers: Digitale Korrelation von Fernerkundungsaufnahmen aus Wattgebieten (to be published)

(4) W.Göpfert: Korrelation komplex exponierter Daten, ZfV 10, 1978